Static Properties of Noninteracting Comb Polymers in Dense and Dilute Media. A Monte Carlo Study

Andreas Gauger and Tadeusz Pakula*

Max-Planck-Institut für Polymerforschung, Postfach 3148, 55021 Mainz, Germany

Received July 8, 1993; Revised Manuscript Received September 30, 1994®

ABSTRACT: We present an application of the cooperative motion algorithm (CMA) to ramified polymers. As a model for so-called comb polymers, we consider a main chain of fixed length to which a various number of side chains of different lengths are anchored. The effect of the molecular architecture on the side and on the main chain is investigated. We consider the two- and the three-dimensional case and compare numerical results obtained in dense melts and dilute solutions. The results show a strong influence of the molecular structure on the properties of the main chain. Initially Gaussian chains stretch and become non-Gaussian and non-Markovian. The side chains remain randomly coiled in three-dimensional melts and stretch slightly in two dimensions and in three dimensional solutions.

1. Introduction

Comb polymers consisting of one main chain and many side-chain branches distributed equidistantly along the main chain constitute a specific class of polymers with complex topology. They have been synthesized in various forms and various chemical constitutions.[1] Such molecules may show interesting properties such as microphase separation between the main and the side chains or mesogenic ordering of either the main or the side chain. In spite of a huge amount of literature dealing with such systems, relatively little is known about the structure of the comb molecules in nonordered melts and in solutions. Experimental studies in this field appear to have been so far very scarce except for a very few model branched polymers[2−8] and some starlike polymers.[9−11] Theoretical considerations of molecules with a complicated architecture turn out to be very difficult, if one wants to include excluded volume interactions. These interactions are not taken into account in any of theoretical models for branched polymers presented so far in the literature.[12−16] We therefore would like to study the behavior of idealized comb polymers in various conditions by means of a computer simulation. Some simulations of comb polymers have been reported earlier but only for single chains.[17,18]

In this paper, the simplest case of comblike molecules will be considered, namely athermal systems where no specific interactions between the main and the side chains (except excluded volume) will be taken into account. Dense systems representing melts (with polymers feeling the space completely) or solutions (polymers immersed in a solvent) are considered. The polymers are characterized by three parameters: length of the main chain N_m, length of side chains N_s, and the number of side chains relative to the length of the main chain ϱ_g (grafting density). Depending on these parameters the structure of comb polymers can be varied considerably ranging between linear polymers (with N_m large and N_s or ϱ_g very small) on one hand and starlike polymers (with N_m small and N_s or ϱ_g large) on the other hand. We investigate the influence of the polymer architecture (changing the number of side chains and their length) on the structure of the main chain, the side chain, and the whole molecule.

2. The Model

As usual in lattice simulations, polymers are modeled as connected beads on a lattice. Here we use a fcc lattice with coordination number $z = 12$ and a triangular lattice with $z = 6$. As already mentioned this paper deals with ramified polymers. The number of branches coming out of one lattice point is limited by the coordination number. Qualitatively, it is easy to imagine, that a high number of branches hinders the motion of the bead where these branches are connected. Therefore, in this work, the maximum number of branches at one lattice site was limited to 4. We consider polymers composed of one main chain of length N_m. To this main chain we anchor n_s side chains of length N_s. The total degree of polymerization of the molecule is

$$N = N_m + n_s N_s \tag{1}$$

It is convenient to define a grafting density ϱ_g as

$$\varrho_g = n_s/N_m \tag{2}$$

All results shown here were obtained holding N_m constant and equal to 20, whereas ϱ_g and N_s were varied. The range of the side chain length is $1 \le N_s \le 50$. The grafting density ϱ_g was varied between $\varrho_g = 0.25$ (which means one side chain every four monomers of the main chain) and $\varrho_g = 2$ (which means two side chains per monomer of the main chain). Figure 1 shows molecules on a two-dimensional triangular lattice with $N_m = 20$, $N_s = 2$, and $\varrho_g = 1$, as an example. Note that the side chains are, for the sake of simplicity, always distributed regularly along the main chain. In some of the results presented below, results for linear, nonramified chains are included for comparison. They will be denoted as $\varrho_g = 0$ or $N_s = 0$.

In the following, we shall denote the total number of chains in the simulation box as n, and the total number of available lattice sites as n_0. This work shall be restricted to the athermal case. This means that the only interaction considered is the excluded volume interaction. It is taken into account by the fact that no lattice point will be occupied by more than one monomer. We shall consider two different polymer densities

* To whom correspondence should be sent.

® Abstract published in *Advance ACS Abstracts*, November 15, 1994.

0024-9297/95/2228-0190$09.00/0

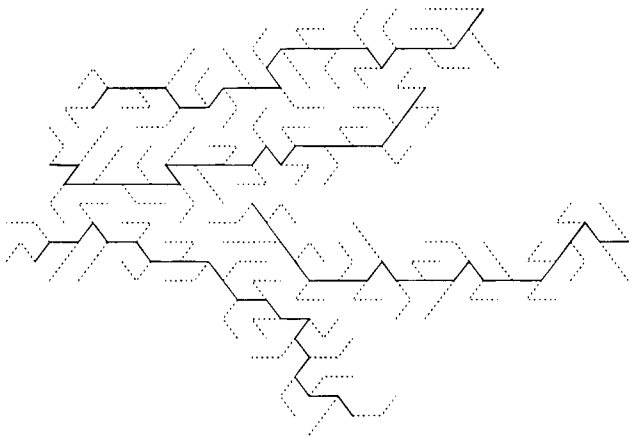

Figure 1. Examples of a comb polymer with $N_m = 20$, $N_s = 2$, $\varrho_g = 1$. The side chains are shown with dotted lines.

$$\varrho = \frac{nN}{n_0} \tag{3}$$

The first one ($\varrho = 1$) models the conditions of a dense polymer melt. The total number of chain monomers is equal to the number of available lattice sites. The second chosen density ($\varrho = 0.05$) is supposed to model a dilute solution. The $(1 - \varrho)n_0$ lattice points which are not occupied by polymer, will be occupied by solvent molecules. The solvent molecules can move freely through the lattice. There will be no interaction, except excluded volume, between the solvent molecules and the polymer. Physically, this means that we consider the case of a good solvent. In order to reduce boundary effects, periodic boundary conditions in all directions were used.

3. The Algorithm

Throughout this investigation, the cooperative motion algorithm (CMA)[19] was used. It is the only lattice algorithm, at the moment, able to simulate monodisperse polymer systems at a density of unity, i.e. every lattice site being occupied by a monomer. When every lattice site is occupied by a monomer, movements involving only the transport of one bead to another lattice point become impossible because of the excluded volume condition. To overcome this shortcoming, the fundamental idea in the CMA is to move beads cooperatively along a closed path in the lattice.[19,20] Each monomer replaces its nearest neighbor along this path. The method was shown to fulfil the principle of detailed balance.[21] As for all other algorithms dealing with many chain systems, ergodicity has not been proven in general, however, for the case of a single chain[22] and for a simulation of a dense dimer system a rigorous proof of ergodicity was given in ref 23. Up to now, the CMA was used to simulate athermal linear and ring polymers,[24,25] stiff polymers,[26] and AB-block copolymers.[27,28] The high efficiency of the method[21] allowed canonical simulations of complicated systems such as mixtures and copolymer melts. A recent review of the principles of the method and its applications to linear molecules is given in ref 28. Here the method is extended to so-called comb polymers presented in the previous section. The basic ideas of the algorithm remain unchanged; some straightforward modifications are needed in the implementation of such a generalization on a computer.

4. Calculated Quantities

In the bulk containing n polymers, each consisting of N beads, the lattice coordinates are mapped on real space coordinates, by taking into account the periodic boundary conditions. The real space coordinates of each monomer are denoted as

$$\vec{r}(i,j) = \vec{e}_x x(i,j) + \vec{e}_y y(i,j) + \vec{e}_z z(i,j) \qquad i = 1, ..., n, j = 1, ..., N \tag{4}$$

where $\vec{e}_x$, $\vec{e}_y$, $\vec{e}_z$ are unit vectors of an orthonormal coordinate system fixed in space.

The center of gravity of polymer i is

$$\vec{R}_{cg,tot}(i) = \frac{1}{N}\sum_{j=1}^{N} \vec{r}(i,j) \tag{5}$$

The center of gravity of the main chain $\vec{R}_{cg,m}$ or the side chain $\vec{R}_{cg,s}$ may be defined in the same way. The average squared radius of gyration of the whole molecule is

$$R_{g,tot}^2 = \frac{1}{nN}\sum_{i=1}^{n}\sum_{j=1}^{N} (\vec{r}(i,j) - \vec{R}_{cg,tot})^2 \tag{6}$$

The quantity g(whole molecule) $= R_{g,tot}^2/R_{g,lin}^2$ is used to characterize the change of size of the comb polymer with respect to the size of the linear chain ($R_{g,lin}^2$) with corresponding molecular mass. Similar definitions hold for the radius of gyration of the main and the side chains, $R_{g,m}^2$ and $R_{g,s}^2$, respectively and consequently the dimensionless ratios g(main chain) $= R_{g,m}^2/R_{g,l}^2$ and g(side chain) $= R_{g,s}^2/R_{g,l}^2$ are used to characterize changes of chain sizes with respect to sizes of equivalent linear chains. The quantities $R_{g,m}^2$ and $R_{g,s}^2$ will of course be calculated respective to the centers of gravity $R_{cg,m}$ $\vec{R}_{cg,m}$ and $\vec{R}_{cg,s}$ of the main and side chains, respectively. Furthermore, mass distributions in a principal axis coordinate frame tied to each polymer will be considered. To this aim, a coordinate frame is assigned to each sampled polymer, with the z axis aligned parallel to the end-to-end vector of the main chain, and the origin placed at the center of gravity $\vec{R}_{cg,tot}$ of the selected molecule. While the z axis is fixed by the direction of the end-to-end vector, the x axis is each time chosen randomly in a direction perpendicular to the z axis. Then the y axis is determined by the two previously chosen axes. Let us denote the coordinates of the beads of this special polymer by

$$x'(i),y'(i),z'(i) \qquad i = 1, ..., N \tag{7}$$

Interesting quantities characterizing the shape of molecules are now the components of the moment-of-inertia tensor, especially the diagonal components

$$R_{g,tot,p}^2 = \frac{1}{N}\sum_{i=1}^{N} z'^2(i)$$
$$R_{g,tot,s}^2 = \frac{1}{N}\left(\sum_{i=1}^{N} x'^2(i) + \sum_{j=1}^{N} y'^2(j)\right) \tag{8}$$

In the same way, we may define the quantities $R_{g,m,p}^2$ and $R_{g,m,s}^2$ for the main chain. Consider two bonds $\vec{a}(i),\vec{a}(i+n)$ belonging to two monomers of the same chain, separated by n bonds of this chain. We define the bond–bond correlation function $C_{bb}(n)$ as the average

$$C_{bb}(n) = \langle \vec{a}(i)\cdot\vec{a}(i+n) \rangle \tag{9}$$

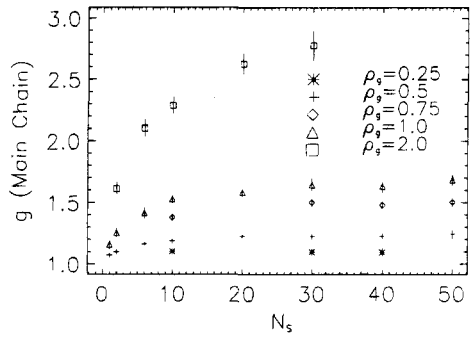

Figure 2. The ratio g(main chain) = $R_{g,m}^2/R_{g,l}^2$ versus side chain length N_s for various grafting densities ϱ_g.

over all possible pairs of bonds separated by n other bonds. We shall normalize C_{bb} in a way that

$$C_{bb}(0) = 1 \tag{10}$$

As a measure of the chain stiffness, we consider the so-called persistence length l_p, which is defined as

$$l_p = 1 + \sum_{n=1}^{N} C_{bb}(n) \tag{11}$$

5. Results in the Dense Melt

5.1. Main Chain. We investigate the influence of an increasing grafting density and side chain length on the conformation of the main chain. Figure 2 shows the ratio g(main chain) of the squared radius of gyration of the main chain in the comb polymer and of the corresponding unperturbed linear chain versus the side chain length. It is seen that increasing grafting density and increasing side chain length cause an extension of the main chain. This can be explained with the effect of the excluded volume condition. Two neighboring side chains will repel each other. Therefore their grafting points at the main chain will also repel one another and the main chain stretches. For large N_s there seems to be a saturation effect. It might be related to the fact, that in three dimensions the outer monomers of the side chains find enough space to arrange almost freely. Therefore only inner monomers conflict strongly with one another and contribute to the stretching effect. The length of the side chain needed to reach the saturation regime is strongly influenced by the grafting density. For $\varrho_g = 0.25$ the saturation seems to be reached already for $N_s = 10$ while for $\varrho_g = 2$ it could not be reached with $N_s = 30$. Note that longer side chains seem to be out of range at the moment, as the total degree of polymerization N for $\varrho_g = 2$ and $N_s = 30$ is already $N = 1220$. Larger molecules can not be handled with actual computer power. On the other hand, when the length of side chains exceed the length of the main chain, the polymer should rather be considered as starlike and not as a comblike.

On a more local scale of the main chain, let us consider the bond–bond correlation function C_{bb} defined in (9). The decay of C_{bb} is shown in Figure 3 for N_s = 20 and various grafting densities. The fact that C_{bb} decays slower and slower as the grafting density is increased, shows that the chains become stiffer and stiffer on a local scale. On the other hand, for so-called Markovian chains, it is easy to show that the bond–bond correlation should decay exponentially with increasing n. This fact was shown in previous simulations

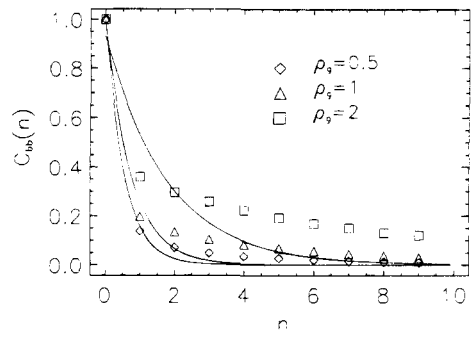

Figure 3. Plot of the bond–bond correlation function $C_{bb}(n)$. The full curves show exponential decays.

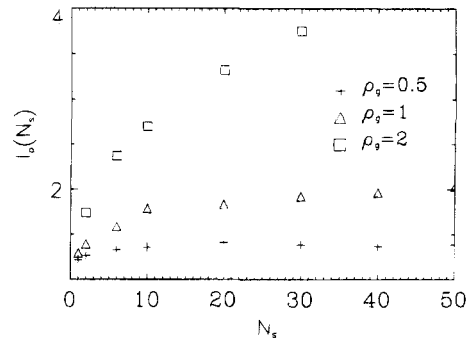

Figure 4. Persistence length l_p of the main chain versus side chain length N_s for various grafting densities ϱ_g.

of flexible and stiff chains.[28] In this case,[28] stiffness of the chain was modeled by so-called bond–angle potentials. Here, we have stiffness of the main chain caused by excluded volume interactions with the side chains. As Figure 3 clearly shows, the exponential decay does not fit at all to C_{bb}. This means that the main chain becomes strongly non-Markovian, as side chains are anchored. There seem to be long-range correlations along the main chain caused by the molecular architecture. Equation 11 defines the persistence length of the main chain. The numerical results are shown in Figure 4. The persistence length shows the same dependence on side chain length and grafting density as the radius of gyration. The saturation effect is seen again for $\varrho_g \leq 1$.

We now come to the anisotropic shape of the main chain. It can be expressed in terms of the ratio

$$Q = R_{g,m,p}^2/R_{g,m,s}^2 \tag{12}$$

For Gaussian chains a value $Q = 2$ is predicted,[30] which is confirmed by simulation results for linear chains in dense melts.[25,28] An increase of Q is the expression of a higher anisotropy of the shape of the chain. For stiff chains modeled via bond–angle potentials we found values ranging between $Q = 2$ and $Q = 2.7$.[28] Figure 5 shows the values obtained for Q in the simulations of comb polymers. The tendency toward a stronger anisotropy with increasing grafting density and side chain length is very pronounced. The maximum values reached ($Q \approx 6$ for $\varrho_g = 2$, $N_s = 30$) are much higher than those obtained previously for stiff chains.[28]

This section has shown that the structure of a linear, Markovian chain with Gaussian properties is strongly influenced, when side chains are anchored. Obviously the chain stretches, as a result of the excluded volume condition. Furthermore nonlocal correlations can be observed and the whole shape of the chain becomes strongly non-Gaussian.

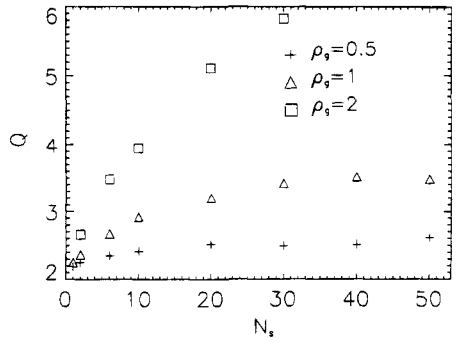

Figure 5. The ratio $Q = R_{g,m,p}^2/R_{g,m,s}^2$ for the main chain versus side chain length N_s for various grafting densities ϱ_g.

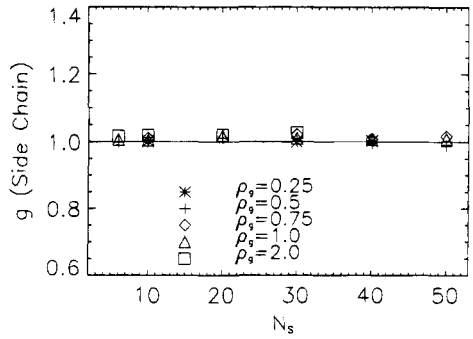

Figure 6. The ratio g(side chain) $= R_{g,s}^2/R_{g,l}^2$ depending on the length N_s of side chains. The different symbols refer to different grafting densities ϱ_g. The full curve represents a scaling function $R_{g,s}^2 \approx N^{1.02}$ ($\varrho_g = 0$).

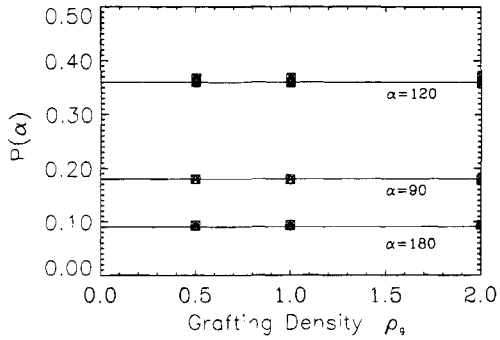

Figure 7. Probabilities $P(\alpha)$ of the bond angles versus the grafting density ϱ_g. Different symbols refer to different side chain lengths N_s. Full curves correspond to the probabilities obtained by the degeneracy degrees.

5.2. Side Chains. Figure 6 shows a plot of the ratio g(side chain) depending on the grafting density of side chains and on their length. The interesting point is the coincidence of the data points for various ϱ_g. It is an interesting finding, that the radius of gyration of the side chains is not influenced by the fact that they are grafted to a main chain. The same result also holds for the persistence length. Another way to visualize that the statistics of the side chains remains unchanged is to look at the distribution of bond angles. The structure of the lattice allows four different bond angles, $\alpha = \pi$, $2\pi/3$, $\pi/2$, $\pi/3$ with degeneracy factor $d(\alpha) = 1, 4, 2, 4$, respectively. For melts of self-avoiding linear chains in the athermal case, it is found[28] that the probabilities $P(\alpha)$ for the bond angles are directly proportional to the degeneracies $d(\alpha)$. In Figure 7 the bond angle probabilities of the side chains are shown for various grafting densities. The data show that the statistics of the side chains are not influenced by the molecular architecture. A similar plot for the main chain would yield a strong influence of the structure of the molecule on the bond angles (not shown). For entropic reasons it seems to be more probable that the main chain loses entropy by stretching out while the side chains remain randomly coiled.

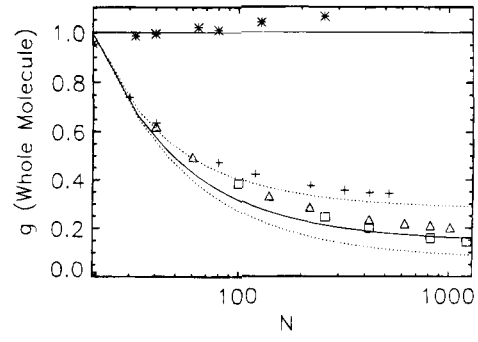

Figure 8. The ratio g(whole molecule) $= R_{g,tot}^2/R_{g,lin}^2$ versus the total degree of polymerization N, for various grafting densities ϱ_g: (*) −0, (+) −0.5, (△) 1.0, and (□) −2.0. The solid and dotted curves are obtained by means of (13) for $\varrho_g = 2$, 1, 0.5, and 0, from the bottom to the top.

5.3. Extension of the Whole Molecule. Several attempts have been made to describe statistical properties of complex branched polymers. All theories, however, disregard the self-avoidance condition and for the type of polymers considered here reduce to the same dependence of the global size of the comb polymer on its structural parameters.[14] According to Zimm and Stockmayer treatment (with the use of Kramers theorem)[12,13] the mean square radius of gyration of ramified polymers (without self-avoidance) can be described by the formula:

$$R_{g,tot}^2 = \frac{b^2}{N^2}\sum_i n_i(N - n_i) \qquad (13)$$

The sum runs over all possibilities i to cut the molecule into two pieces. N is the total degree of polymerization in the molecule, b the bond length, n_i and $N - n_i$ are the numbers of monomers included in the two resulting parts. Consider for example a linear molecule. There are $N - 1$ possibilities to cut the chain into two pieces, and

$$R_{g,tot}^2 = \frac{b^2}{N^2}\sum_{i=1}^{N-1} i(N - i) = \frac{b^2}{N^2}[(N^3/6) + (1/6)] \qquad (14)$$

For large N, the well-known scaling law for the random walk $R_{g,tot}^2 \approx N^1$ is obtained. As already mentioned, Kramer's theorem strictly holds only for non-self-avoiding polymers. On the other hand, it is well known,[31,32] that in dense polymer melts the excluded volume interaction is screened. Therefore, for linear self-avoiding chains in melts the result is correct, one finds the idealized scaling law $R_{g,tot}^2 \approx N$. Section 5.1 showed that in comb polymers the excluded volume interaction is not screened anymore and that it results in a stretching of the main chain. Therefore one cannot expect the formula (13) to be exact any longer. But it is at the moment the only ansatz to describe the extension of ramified polymers. The regular structure of the polymers in the simulation allows an analytical calculation of $R_{g,tot}^2$ with the help of (13). The results are quite lengthy and will not be shown here. Figure 8 shows a comparison between simulated and theoretical ratios g(whole chain), where the points represent simulated results and the lines are calculated using $R_{g,tot}^2$

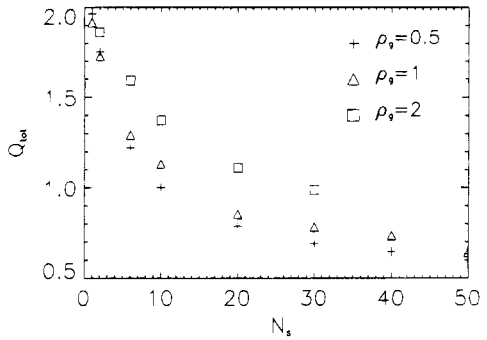

Figure 9. The ratio $Q_{tot} = R_{g,tot,p}^2/R_{g,tot,s}^2$ for the whole molecule versus the side chain length N_s.

given by (13). For the sake of completeness results for linear chains are also included. As expected, the theoretical results hold relatively good for linear chains. Even for $\varrho_g = 0.5$ the agreement remains quite good. But as the grafting density is increased further, there are strong deviations of the simulation results from the theoretical curves. These deviations are caused by the excluded volume interaction. As we have seen in section 5.1, an increase of the grafting density results in an increase of the radius of gyration of the main chain. Therefore, the whole molecule will be somehow blown up, and the simulated values for $R_{g,tot}^2$ are larger than the calculated ones.

Analogous to the results of section 5.1 we now show results for the anisotropy of the whole molecule

$$Q_{tot} = \frac{R_{g,tot,p}^2}{R_{g,tot,s}^2} \tag{15}$$

Figure 9 shows a plot of Q_{tot} versus the side chain length. While Figure 5 showed a dramatic increase of Q for the main chain, we now have a decrease of the anisotropy of the whole molecule. This becomes easy to explain, when one keeps in mind that the side chains are essentially Gaussian and that N_s is of the same order of magnitude than N_m or even larger. With increasing N_s the whole polymer tends to adopt a more and more spherical conformation similar to that of star polymers.

For $\varrho_g \leq 1$, Q_{tot} finally almost reaches a value of 0.5 which is characteristic for the isotropic configuration of starlike chains. The decay from $Q_{tot} = 2$ (Gaussian value for $N_s = 0$) to smaller values at $N_s > 0$ is slower and slower with increasing grafting density. This can be explained by two counteracting effects. On one hand, the main chain is strongly stretched, which increases the anisotropy, on the other hand an increase in N_s tends to lower the anisotropy.

6. Results in Dilute Solution

As already mentioned in section 3, we consider the case of a good solvent, where there is no interaction between the solvent molecules and the polymers. The considered polymer concentration is $\varrho = 0.05$. Section 5.1 showed that the excluded volume interaction cannot be screened totally in melts of comb polymers. It results in a stretching of the main chain. It is well known that for linear chains in dilute solutions the excluded volume interaction has strong effects on the structure of the molecule. They result in a new scaling exponent for the radius of gyration.[31] Thus one can suspect that the effect of the excluded volume combined with the comb polymer architecture may have more dramatic effects

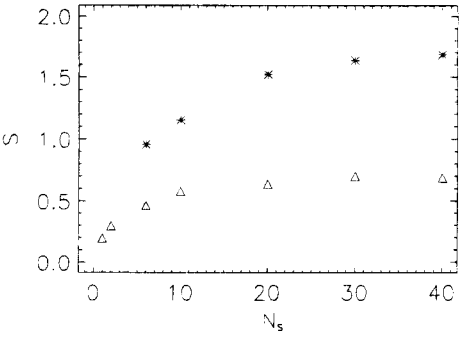

Figure 10. A comparison of the relative stretching $S = [R_{g,m}^2(n_s) - R_{g,m}^2(n_s = 0)]/R_{g,m}^2(n_s = 0)$ in the melt (△) and in dilute solution (*). In both cases the grafting density is $\varrho_g = 1$.

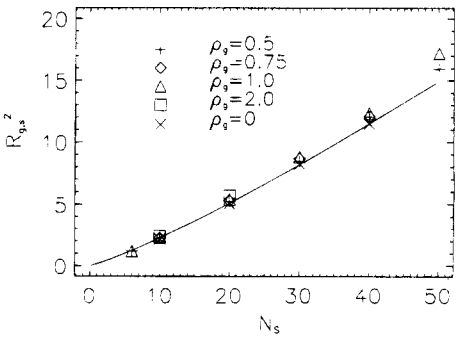

Figure 11. The radius of gyration of the side chains versus their length N_s in dilute solution. The full curve shows the expected scaling law for linear chains $R_g^2 = N^{1.2}$.

in a solution than in a melt. The simulation data show that the effects on the main chain in a solution are qualitatively the same as those presented in section 5.1. To compare the two cases quantitatively let us consider the relative stretching

$$S = \frac{R_{g,m}^2(N_s) - R_{g,m}^2(N_s=0)}{R_{g,m}^2(N_s=0)} \tag{16}$$

A plot of S versus the side chain length is shown for dense and dilute media in Figure 10. In both cases, the considered grafting density was $\varrho_g = 1$. The data show that the effect is much more pronounced in the solution than in the melt. Obviously the effects of the excluded volume interaction remain partially screened in the melt even for the comb polymer architecture. The saturation effect is seen in both cases.

Figure 11 shows the radius of gyration of the side chains for various grafting densities depending on the side-chain length. In the melt, Figure 6 revealed no influence of the molecular architecture on the dimensions of the side chains. Now, in the case of a dilute solution there is a small effect. Especially for large N_s, the radius of gyration $R_{g,s}^2$ increases slightly with increasing grafting density. However, the effect is much less pronounced than the effect on the main chain. The relative stretching of the side chains is around 10%, while it is about 180% for the main chain. The interactions leading to a stretching of the side chain seem to be so small that they can be fully screened in the dense melt.

The results obtained here for comb molecules in solution are qualitatively in agreement with former simulations performed for single chains.[17,18] A precise comparison of these results is, however, difficult because the parameters of systems simulated by different methods do not agree exactly. Nevertheless, we can relate

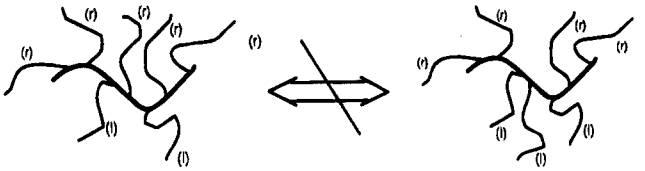

Figure 12. An example for nonergodicity in two dimensions. No algorithm involving only moves of beads to a nearest neighbor place may transport a side chain from one side of the main chain to the other.

our results presented in Figure 10 to these reported by McCrakin and Mazur[17] but obtained for comb polymers at the θ condition. In Figure 11 of their paper,[17] the authors characterized the extension of the backbone as a function of the length of side chains by means of the ratio of the mean squared radius of gyration of the backbone to the radius of gyration of corresponding linear chains. For chains of the same parameters as these considered here in Figure 10, they obtained a dependence which can be regarded as being in quantitative agreement with that presented here for the melt of comb chains. It should be considered as a very satisfactory agreement if we take into account that results of these authors have been obtained for chains under θ conditions. They have also demonstrated (Figure 12 in ref 17) that changing properties of the solvent to a good one will increase the extension of the backbone in a comb polymer. Such an increased extension will lead to a shift of the S vs N_s dependence toward that obtained here for a good solvent (Figure 10). Further agreement between results obtained for side chains under θ conditions and these reported here for the melt can be noticed from a comparison of Figure 11 of ref 17 with Figure 2 of this paper. It indicates that the excluded volume interactions in the θ solution become screened to a comparable extent as in the melt of comb polymers.

7. Results in Two Dimensions

While all results presented thus far were obtained on a three-dimensional fcc lattice, we now turn to a two-dimensional triangular lattice with a coordination number of $z = 6$. Simulations of comb polymers in two dimensions raise a further problem: nonergodicity. As a matter of fact, no algorithm dealing with many chain systems of comb-shaped polymers can be ergodic in two dimensions. A simple example may help to illustrate this statement (Figure 12). Following the main chain contour, one may classify the side chains into two types: (r) those which bifurk to the right side of the main chain and (l) those which bifurk to the left side of the main chain. In any algorithm involving only moves where one bead is transported to a neighboring site, a side chain labeled r can never become labeled l and vice versa. Of course, one could think about transporting the side chain as a whole to the other side of the main chain in one step. Dealing with many chain systems such a procedure would fail, the acceptance rates would be too low due to the excluded volume condition. In three dimensions there is no such problem as the side chains can rotate freely around the main chain. In order to avoid further parameters in the simulation, the side chains will bifurk alternating l and r from the main chain (see Figure 1). All results presented in this section are obtained in the dense limit $\varrho = 1$.

The effect of the molecular architecture on the main chain is the same as in three dimensions. The radius of gyration as well as the persistence length increases with increasing grafting density and side chain length.

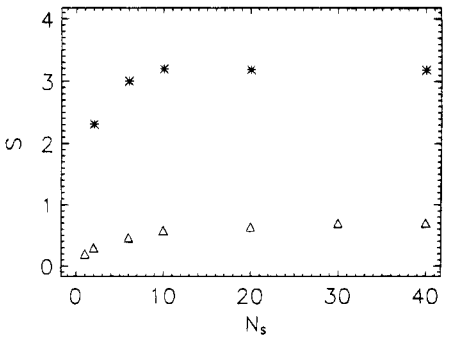

Figure 13. A comparison of the relative stretching $S = [R_{g,m}^2(n_s) - R_{g,m}^2(n_s = 0)]/R_{g,m}^2(n_s = 0)$ in the three (△)- and two-dimensional (*) case. In both cases the grafting density is $\varrho_g = 1$.

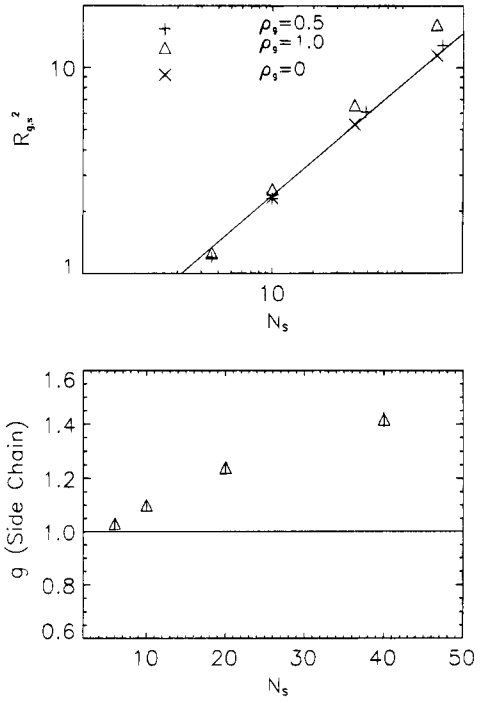

Figure 14. (a) Radius of gyration of the side chains in two dimensions. The full curve shows a fitted scaling law for nonramified chains $R_g^2 \approx N^{1.05}(\varrho_g = 0)$. (b) The ratio g(side chain) vs N_s for $\varrho_g = 1$.

For a quantitative comparison between two and three dimensions, the stretching factor S [see (16)] is plotted in Figure 13 for $\varrho_g = 1$. The figure shows that the stretching in two dimensions is much more pronounced (up to 4 times) than in the three-dimensional case. The mutual hindering of the side and the main chains is very strong due to the smaller number of degrees of freedom.

The problem of the structure of side chains is now distinctly different from that in section 5.2. The side chains are now anchored to a one-dimensional main chain which they can neither cross nor rotate around. Furthermore, they are embedded in a two-dimensional space. The problem for the side chains can therefore be related closely to the two-dimensional brush problem.[33]

For polymers grafted to an impermeable surface, one expects

$$R_g^2 \approx N^2 \tag{17}$$

To see, how to extend such a result to the comb polymer in two dimensions, let us consider some simple scaling

arguments. Consider a main chain with an extension of N_m (we assume for simplicity that it has been fully stretched by the presence of the side chains). Let the extension of the side chains be R. Of course, the side chains are allowed to lie in the same direction than the main chain. The whole space occupied by the molecule is then

$$(N_m + 2R)R \tag{18}$$

If all monomers of the molecule are densely packed in this volume, one obtains

$$(N_m + 2R)R \approx N_m \varrho_g N_s \tag{19}$$

Now, two limiting cases are considered: (1) for $N_m \gg R$ (boundary effects disregarded) one obtains the typical scaling law for polymer brushes $R \approx N_s$; and (2) for $N_m \ll R$ (boundary effects are important) the result for unperturbed chains $R^2 \approx N$ is found.

Of course, in the simulation none of these limiting cases is really reached, we therefore cannot expect a determined scaling behavior of the side chains. Figure 14 shows $R_{g,s}^2$ and the ratio g(side chain) versus the length of side chains. Results for linear chains in two dimensions are also included. In this case, g(side chain) increases with increasing grafting density. The effect is more pronounced than in three-dimensional solutions. However, the relative stretching expressed by Q is much smaller than the stretching of the main chain. In the considered range of side chain length, it could seem as if the scaling law for $\varrho_g = 1$ would be different from the one for linear chains. However, as the simple scaling arguments showed, one expects that for larger N_s (N_m remaining constant), the simple law $R_{g,s}^2 \approx N_s$ is reached. Therefore it makes no sense to claim a new scaling exponent fitted to the available data points.

8. Conclusions

This paper has shown that the cooperative motion algorithm, previously applied to linear chains, can be extended to simulate so-called comb polymers. For simplicity, this work considers only noninteracting (except excluded volume) polymers. It is shown that an originally Gaussian chain acquires strongly non-Gaussian properties, as side chains are anchored. Even the Markovian property is lost and replaced by long-range correlations along the main chain. These results hold for three as well as for two dimensions, in melts and in dilute solutions. They can be explained with the help of the excluded volume interaction.

An interesting result concerning the side chains is that they are only affected by the molecular architecture in two dimensions and in three-dimensional solutions. In three-dimensional melts they remain randomly coiled. This surprising result could be related to the screening of the excluded volume interaction in melts.

The ansatz shown in this work to model and simulate comb polymers turns out to be quite effective concerning the amount of CPU time needed. It is therefore suitable for the modeling of interacting comb polymers. One may, for example, think about introducing repelling interactions between monomers of the side and the main chain. Such interactions should lead to a microphase transition, which has already been considered theoretically for various polymer architectures.[34,35] Canonical simulations of such a transition have given interesting results and will be presented elsewhere.[36]

References and Notes

(1) Plate, N. A.; Shibaev, V. P. In "Comb-shaped polymers an Liquid crystals"; Plenum Press: New York, 1987.
(2) Noda, I.; Horikawa, T.; Kato, T.; Fujimoto, T.; Nagasawa, M. *Macromolecules* **1970**, *3*, 795.
(3) Roovers, J. E. L. *Polymer* **1975**, *16*, 827.
(4) Roovers, J. *Polymer* **1979**, *20*, 843.
(5) Roovers, J.; Toporowski, P. M. *J. Polym. Sci. Polym. Phys. Ed.* **1980**, *18*, 1907.
(6) Tsukahara, Y.; Mizumo, K.; Segawa, A.; Yamashita, Y. *Macromolecules* **1989**, *22*, 1546.
(7) Siochi, E. J.; De Simone, J. M.; Hellstern, A. M.; McGrath, J. E.; Ward, T. C. *Macromolecules* **1990**, *23*, 4696.
(8) Ilto, K.; Tomi, Y.; Kawaguchi, S. *Macromolecules* **1992**, *25*, 1534.
(9) Khasat, N.; Pennisi, R. W.; Hadjichristidis, N.; Fetters, L. J. *Macromolecules* **1988**, *21*, 1100.
(10) Bauer, B. J.; Fetters, L. J.; Gressley, W. W.; Hadjichristidis, N.; Quack, N. G. F. *Macromolecules* **1989**, *22*, 2337.
(11) Horton, J. C.; Squires, G. L.; Boothroyd, A. T.; Fetters, L. J.; Rennie, A. R.; Glinka, C. J.; Robinson, R. A. *Macromolecules* **1989**, *22*, 681.
(12) Kramers, H. A. *J. Chem. Phys.* **1946**, *14*, 415.
(13) Zimm, B. H.; Stockmayer, W. H. *J. Chem. Phys.* **1949**, *17*, 1301.
(14) Kurata, M.; Fukatsu, M. *J. Chem. Phys.* **1964**, *41*, 2934.
(15) Casassa, E. F.; Berry, G. C. *J. Polym. Sci. Part A-2* **1966**, *1*, 331.
(16) Glinka, H. *Macromolecules* **1983**, *16*, 1479.
(17) McCrackin, F. L.; Mazur, J. *Macromolecules* **1981**, *14*, 1214.
(18) Lipson, J. E. G. *Macromolecules* **1991**, *24*, 1327.
(19) Pakula, T. *Macromolecules* **1987**, *20*, 679.
(20) Pakula, T.; Geyler, S. *Macromolecules* **1988**, *21*, 1665.
(21) Reiter, J.; Edling, T.; Pakula, T. *J. Chem. Phys.* **1990**, *93*, 837.
(22) Reiter, J. *Macromolecules* **1990**, *23*, 2811.
(23) Reiter, J. *Phys. A* **1993**, *196*, 149.
(24) Geyler, S.; Pakula, T. *Makromol. Chem. Rapid Commun.* **1988**, *9*, 617.
(25) Pakula, T. *J. Chem. Phys.* **1991**, *95*, 4685.
(26) Gauger, A.; Pakula, T. *J. Chem. Phys.* **1993**, *98*, 3548.
(27) Weyersberg, A.; Vilgis, T. A. *Phys. Rev. E* **1993**, *48*, 377.
(28) Gauger, A.; Weyersberg, A.; Pakula, T. *Makromol. Chem., Theory Simul.* **1993**, *2*, 531.
(29) Yamakawa, H. In *Modern Theory of Polymer Solutions*; Harper and Row: New York, 1971.
(30) Flory, P. J. In *The Principles of Polymer Chemistry*; Cornell University Press: Ithaca, NY, 1953.
(31) Edwards, S. F. *J. Phys. A* **1975**, *8*, 1670.
(32) Alexander, S. *J. Phys. Fr.* **1977**, *38*, 983.
(33) Leibler, L. *Macromolecules* **1980**, *13*, 1602.
(34) de la Cruz, M. O.; Sanchez, I. C. *Macromolecules* **1988**, *19*, 2501.
(35) Gauger, A.; Pakula, T. Submitted to *Macromolecules*.

MA941015I